Monthly Notices
of the
ROYAL ASTRONOMICAL SOCIETY

MNRAS **437,** 1828–1835 (2014)
Advance Access publication 2013 November 14

doi:10.1093/mnras/stt2011

ExoMol line lists – III. An improved hot rotation-vibration line list for HCN and HNC

R. J. Barber,[1] J. K. Strange,[1] C. Hill,[1] O. L. Polyansky,[1] G. Ch. Mellau,[2] S. N. Yurchenko[1] and Jonathan Tennyson[1]★

[1]*Department of Physics and Astronomy, University College London, London WC1E 6BT, UK*
[2]*Physikalisch-Chemisches Institut, Justus-Liebig-Universität Giessen, Heinrich-Buff-Ring 58, D-35392 Giessen, Germany*

Accepted 2013 October 17. Received 2013 October 15; in original form 2013 September 9

ABSTRACT

A revised rotation-vibration line list for the combined hydrogen cyanide (HCN)/hydrogen isocyanide (HNC) system is presented. The line list uses ab initio transition intensities calculated previously and extensive data sets of recently measured experimental energy levels. The resulting line list has significantly more accurate wavelengths than previous ones for these systems. An improved value for the separation between HCN and HNC is adopted, leading to an approximately 25 per cent lower predicted thermal population of HNC as a function of temperature in the key 2000 to 3000 K region. Temperature-dependent partition functions and equilibrium constants are presented. The line lists are validated by comparison with laboratory spectra and are presented in full as supplementary data to the article and at www.exomol.com.

Key words: molecular data – opacity – astronomical data bases: miscellaneous – planets and satellites: atmospheres – stars: low-mass.

1 INTRODUCTION

Hydrogen cyanide (HCN) and its higher energy isomer hydrogen isocyanide (HNC) are well known in a number of astrophysical environments. For example, they are both prevalent in interstellar clouds where HNC, despite lying at much higher energy, is often observed to be of similar abundance as HCN (Hirota et al. 1998). HCN and HNC are also observed well-outside thermodynamic equilibrium in cometary atmospheres (Hirota et al. 1999) for which detailed spectroscopic models are being developed (Lippi et al. 2013). Non-thermal HCN is also found on Titan where it is an important coolant (Rezac et al. 2013). In cool stars, where the two isomers exist in thermodynamic equilibrium, it has been suggested their abundance ratio should act as a thermometer (Harris et al. 2003).

In fact the opacity of HCN has a dramatic influence on the atmospheres of cool carbon stars. Eriksson et al. (1984) showed that the inclusion of an HCN line list (Jørgensen et al. 1985) resulted in models for the atmospheres of cool carbon-rich stars in which the modelled atmosphere expanded by a factor of 5 and the gas pressure of the surface layers was lowered by one or two orders of magnitude. This clearly illustrates the importance of accurate HCN opacities for such models. Similarly, HCN spectra have been observed in T Tauri stars (Carr & Najita 2011), extragalactic red giants (van Loon et al. 2006) and have been used to constrain C and N abundances in AGB stars (Matsuura et al. 2005).

Neither HCN nor HNC has so far been detected in the atmospheres of exoplanets. However HCN is predicted to be an important species and a possible sighting has recently been claimed (Oppenheimer et al. 2013). HCN is likely to feature in carbon-rich atmospheres, especially so when disequilibrium effects are taken into account (Madhusudhan 2012; Venot et al. 2012; Moses et al. 2013). Indeed, surprise has been expressed that HCN has yet to be firmly observed in exoplanets (Moses 2013). HCN is thus a key species for proposed exoplanet characterization studies (Tinetti et al. 2012). This work, along with the other studies cited above, requires accurate spectroscopic data for the HCN system.

Eriksson et al. (1984) computed a comprehensive vibration-rotation line list using an ab initio quantum chemical procedure (Jørgensen et al. 1985). This line list was an important step forward but is not particularly accurate and did not include any contribution from HNC. Harris, Polyansky & Tennyson (2002b) computed a new and even more extensive vibration-rotation line list which covered both HCN and HNC. This work was again based on ab initio quantum chemistry (van Mourik et al. 2001) which was shown to reproduce laboratory spectra with reasonable accuracy (Harris, Polyansky & Tennyson 2002a). However, this line list, designated HPT below, is far from spectroscopic accuracy. Harris et al. (2006) tried to improve the accuracy of the line list by shifting the calculated energy levels to ones measured experimentally, a procedure similar to that employed below. However this effort was hampered

★E-mail: j.tennyson@ucl.ac.uk

by the lack of laboratory data, particularly for levels important when the system is hot, so that only 5200 energy levels were shifted. Harris et al. (2008) used a similar technique to generalize the HPT line list to the $H^{13}CN$ system.

Since the work of Harris et al. (2006), Mellau has performed systematic experimental studies on the hot emission spectra of both HCN (Mellau, Winnewisser & Winnewisser 2008; Mellau 2011a,b,c) and HNC (Mellau 2010a,b, 2011d). This has led to the experimental determination of over 40 000 rotation-vibration energy levels of this system. Experimental energy level lists are provided in the Supplementary Material of these papers (Mellau 2010a,b, 2011a,b,c,d). Up to 7000 cm^{-1} above the HCN ground state and for 4000 cm^{-1} above the HNC ground state, Mellau's energy level list is complete and high-resolution accurate. This complete list gives the first practically error-free partition function at room temperature for a polyatomic molecule. For the range of 7000–9000 cm^{-1} above the HCN ground state and 4000–6000 cm^{-1} above the HNC ground state a complete preliminary energy level list was computed by Mellau. The energy level list in this region combines the experimental energy levels with predicted energy levels. For the vibrational states not covered by measurements, accurate global predictions of the spectroscopic constants have been used to calculate the energy levels. For each vibrational state, the experimental energy levels are directly related to measured transitions only for a given J_{max}. The energy levels for each vibrational state have been extended up to $J = 90$ for HCN and up to $J = 70$ for HNC with calculated energy levels based on the spectroscopic constants determined using transitions up to J_{max}.

In this work, we merge Mellau's experimental and predicted energy level list with a modified HPT line list corrected for a more accurate position of the HNC minimum to provide a substantially improved single combined line list. Based on these data, we give improved partition functions for high-temperature applications.

The relative accuracies of energy level measurements are usually so high that even if the relative error of the ab initio energy levels are of the order of 10^{-3} to 10^{-4}, they are many orders of magnitude worse than experimental data. In the case of line intensities, high-resolution accuracy means experimental line intensities accurate to only to 1–10 per cent. Due to this discrepancy, intensities derived from ab initio calculations are much more comparable with measurements than is the case for the ab initio frequencies. This work relies heavily on the assumption that ab initio transition intensities computed in the original HPT line list are reliable. Mellau's group have performed extensive band intensity analysis in the ν_1 frequency region based on intensity calibrated emission spectra. In this study, they found an excellent agreement between the measured and HPT line intensities up to a relatively high bending excitation of $v_2 = 7$. This conclusion is supported by comparisons with Mellau's laboratory emission spectra in the ν_2 bending region we give below, and by experience with similar calculations on other molecules (Lynas-Gray, Miller & Tennyson 1995; Lodi, Tennyson & Polyansky 2011).

The current work forms part of the ExoMol project. This project aims to provide line lists of spectroscopic transitions for key molecular species which are likely to be important in the atmospheres of extrasolar planets and cool stars; its aims, scope and methodology are summarized in Tennyson & Yurchenko (2012). This paper is third in series of line list studies performed as part of this project. The previous studies concerned the diatomic species BeH, MgH and CaH (Yadin et al. 2012), and SiO (Barton, Yurchenko & Tennyson 2013).

2 METHOD

2.1 Spectroscopic data

The Harris et al. (2002b, HPT) line list consists of two files, one containing the energies of the eigenstates and their rotational and vibrational quantum numbers, where known (the states file), and the other a list of allowed transitions between these states (the transitions file). The list with the energies of the eigenstates contains 168 110 entries, of which 22 702 have rovibrational assignments. HPT considers rotationally excited states with J up to 60.

Mellau's HCN experimental data set contains the eigenenergy for 26 344 eigenstates, of which 14 690 (55.8 per cent) are '*e*' parity and 11 654 are '*f*' parity. These states correspond to 218 vibrational '*e*' or '*f*' sublevels determined from the analysis of the emission spectra and to 82 '*e*' or '*f*' sublevels calculated using predicted spectroscopic constants. All sets have been extended using spectroscopic predictions from the J_{max} reported (Mellau et al. 2008; Mellau 2011a,b,c) up to $J = 90$. The HNC data set contains 14 284 HNC eigenstates, of which 8136 (57.0 per cent) are '*e*' parity and 6148 are '*f*' parity. The HNC data set has 210 sets of vibrational '*e*' or '*f*' sublevels; each set is extended from the reported J_{max} value (Mellau 2010a,b, 2011d) up to $J = 70$.

As we place HCN and HNC levels on a single energy scale, it is necessary to align them both by allowing for the energy of moving from HCN to HNC and by using a common cut-off for the levels of the two isomers. The energy of the highest assigned HNC level in Mellau's experimental data is at 16 000 cm^{-1} above the HCN ground state. As the highest assigned HNC level in the HPT list is 10 000 cm^{-1} below this limit, only HNC levels in the experimental list with an energy less than 6000 cm^{-1} above the HNC ground state were considered in this work. This reduced the number of experimental HNC data to be examined to 2001 '*e*' states and 1471 '*f*' states. That is to say, of approximately 30 000 experimental energy levels examined about 88 per cent were for HCN and 12 per cent for HNC. Moreover, relative to their respective ground state energies, the HNC levels were at lower energies. It is for this reason that in our reconstructed line list 15 201 HCN states were substituted, but only 3979 HNC states.

HPT took the isomerisation energy from HCN to HNC from the calculations of van Mourik et al. (2001) which places the HNC ground state 5185.637 cm^{-1} above that of HCN. At present there is only a highly inaccurate experimental determination of the separation between the HCN and HNC ground states (Pau & Hehre 1982), so Mellau's data give the energies of the HNC states relative to the HNC ground state. Hence, in order to make experimental HNC energies comparable with those in the HPT list, it is necessary to increase them by the energy difference between the HNC and HCN ground states. More recent calculations suggest the value for this difference computed by van Mourik et al. (2001) should be somewhat higher (Dawes, Wagner & Thompson 2009). We therefore undertook new calculations at the all-electron multireference configuration interaction level of theory using a large basis set (aug-cc-pCV6Z) and an extended active space for the electron correlation; relativistic and adiabatic corrections were also included. Full results of these calculations will be presented elsewhere. These studies give an isomerisation energy of 5705 $\pm$ 20 cm^{-1}, including allowance for the zero-point energy corrections.

The energies of the HNC levels in HPT were increased by 5705 – 5185.637 = 519.363 cm^{-1} and those from experimental HNC data by 5705 cm^{-1}. The HNC ground state correction can be made only for the rotational manifold of the first 40 HNC

vibrational states labelled as HNC isomer in the HPT list. The correction has consequences for the low- and medium-temperature partition function of the system and the HCN/HNC equilibrium value which are discussed below. In an overall HCN/HNC opacity simulation using the corrected line list, some minor artefacts are expected for HNC transitions between corrected and uncorrected levels.

2.2 The new energy file

Due to the difference in the accuracy of the ab initio and measured eigenenergy data sets the bijective mapping of these data sets is straightforward only up to the fundamental vibrational excitation. Even at relatively low vibrational excitation it becomes increasingly complicated to map these data sets. As the density of states becomes an order of magnitude higher than the difference between measured and calculated eigenenergy values such mapping can be done only by labelling the ab initio eigenenergies with approximate vibrational quantum numbers and isomer labels. From the 168 110 eigenenergies of the HPT list 18 723 are identified as HCN and 3979 as HNC. The remaining 145 408 states have rotational quantum numbers and parities, but the vibrational quantum numbers and the isomeric form are not known. 56.4 per cent of all the states identified are '*e*' parity and 43.6 per cent are '*f*' parity. The assignment was done before Mellau's list became available based on the sparse experimental data available at that time and on the rovibrational structure of the eigenenergies typical for a linear molecule. Mellau's measured and predicted list covers most of these assigned states. To check for possible errors in the original HPT assignment an experimental to ab initio mapping procedure was used in this work.

The isomer code (0 for HCN, 1 for HNC), the parity (1 for '*e*' and 0 for '*f*' states) and the rotational and vibrational quantum numbers for each entry in HPT states file were concatenated and tabulated against the entry number in the file and the energy of the state. Similarly, the experimental data which are organized by vibrational quantum number were rearranged to match the HPT layout, and the isomer code, parity, and rotational and vibrational quantum numbers were concatenated and tabulated against energy. Matching entries were identified by using a simple look-up technique that enabled the experimental energies for the corresponding states to be matched against the HPT entries. The data were then re-arranged according to vibrational quantum numbers and in ascending J values within each vibrational state. Finally, the difference between the HPT energy and experimental energy was computed for each entry.

These differences found were systematic and made it easy to predict the energy of the next highest J with a high degree of accuracy (typically to within 0.1 cm^{-1}). This enabled entries that had been wrongly assigned in the HPT list to be readily identified. Moreover, since the J values are known to be correct and the energies of the state corresponding to the wrongly assigned vibrational quantum numbers must be in the same energy region, by sorting all the levels that had been identified as mislabelled by J and then by energy, it was easy to identify pairs of eigenstates whose quantum numbers had been wrongly assigned. Sometimes the confusion was identified as being between three states with similar energies and on several occasions four nearby states were found to all have quantum numbers belonging to other members in the group. We found 302 HCN states that have been wrongly assigned in HPT. For values of $J < 8$, no wrong assignments were identified. In the range $J = 8$–23 and $J = 50$–60, four or fewer states were found to be wrongly assigned in the HPT list for each value of J, whilst in the region $J = 24$–49, with the exception of $J = 27$ (where there were only four wrong assignments), each value of J had between 6 and 13 states that were wrongly assigned. In the case of HNC, which as mentioned included far fewer states, no meaningful analysis of the misassignments was possible, other than to point out that all the wrongly labelled states were of '*f*' parity.

Next we substituted the experimental energies into the HPT list by matching the quantum numbers. In total, the energies of 15 201 HCN states were replaced with experimental energies, and of these 8544 were '*e*' parity and 6657 '*f*' parity. The energies of 3979 HNC states were replaced with experimental energies, of which 2325 were '*e*' states and 1654 '*f*' states.

An examination of the HPT and experimental data revealed that the principal source of discrepancy between the two sets of data is related to the vibrational band origins. Table 1 details 146 vibrational band origins for the HCN species, arranged by reducing value of the parameter $E_{\mathrm{Expt}} - E_{\mathrm{HPT}}$. The difference in band origins has a strong vibrational angular momentum dependence as shown in fig. 2 of reference Mellau (2011b). The 21 bands showing the greatest difference between the HPT and Mellau energies are highly excited bends with the vibrational angular momentum l values very much lower than quanta of bending vibration, v_2.

Within each band there was also a small systematic change (usually an increase) in the difference between the two sets of energy with increasing values of J. However, the differences due to small changes in J were generally of second order compared to the differences in band origins.

The HPT line list contains the rovibrational assignment of 200 vibrational states, this is 8 per cent of the states below the first isomerisation state. Mellau assigned the rotational manifolds for more than 4000 vibrational states of the HPT line list based on spectroscopic models (Mellau 2011b). Mellau's assignments agree for the first 71 vibrational states with the assignments reported in this work for all rotational states up to $J = 60$. For each of these states, the experimental eigenenergies have been reported up to $J = 60$ (Mellau 2011b) and are included in the line list reported in this work. This means that using the line list reported in this work it is possible to make highly accurate simulations for *any* band between these 71 vibrational states up to $J = 60$. For the next 130 vibrational states, there are differences between these two assignments mainly for highly excited rotational states with $J > 35$. Altogether 5000 of the HPT states have different vibrational label in Mellau's assignment. The band centres of the two assignments match for all 265 different vibrational states including the further 65 highly excited vibrational states assigned only up to $J = 5$–15 in the HPT line list.

2.3 Partition function

We recomputed the temperature-dependent partition function for the two forms of the molecule: HCN and HNC, and produced eighth-order polynomial fits to the data. The results for both HCN and HNC (relative to its own ground state) are very close to those in Barber, Harris & Tennyson (2002), and hence are not reproduced here in tabular form.

For ease of use, we fitted our partition function, Q, to a series expansion of the form used by Vidler & Tennyson (2000)

$$\log_{10} Q(T) = \sum_{n=0}^{8} a_n \left[\log_{10} T\right]^n \quad (1)$$

with the values given in Table 2.

Table 1. Differences in the band origins between the experimental (Expt) values of Mellau and HPT line list, given as observed minus calculated (O − C); all values in cm^{-1}.

Expt	v_1	v_2	ℓ	v_3	O − C	Expt	v_1	v_2	ℓ	v_3	O − C	Expt	v_1	v_2	ℓ	v_3	O − C
6519.610	2	0	0	0	+6.11	4994.340	0	7	5	0	−3.43	6469.266	0	9	7	0	−10.40
9030.994	1	8	8	0	+4.62	2893.589	0	4	4	0	−3.46	8681.197	1	8	0	0	−10.47
8296.128	1	7	7	0	+4.00	1411.413	0	2	0	0	−3.50	3525.720	0	2	2	1	−11.00
3311.477	1	0	0	0	+3.73	5580.396	0	5	1	1	−3.54	4248.567	0	3	3	1	−11.26
6712.451	1	5	1	0	+3.33	5414.442	1	3	3	0	−3.63	8144.625	1	1	1	2	−11.26
6757.336	1	5	3	0	+3.29	9258.983	2	1	1	1	−3.64	5550.442	0	8	2	0	−11.37
6036.960	1	4	0	0	+3.24	4888.039	0	4	0	1	−3.72	7800.933[a]	0	8	6	1	−11.91
9190.518	2	4	2	0	+3.14	2096.846	0	0	0	1	−3.74	5525.813	0	8	0	0	−11.95
6060.819	1	4	2	0	+3.00	714.936	0	1	1	0	−3.86	6270.582	0	3	1	2	−12.30
9167.088	2	4	0	0	+3.00	9459.164	1	6	2	1	−4.01	9469.617	1	9	5	0	−13.56
5881.617	0	8	8	0	+2.98	8563.197	2	3	3	0	−4.07	4881.210	0	1	1	2	−13.61
5125.394	0	7	7	0	+2.59	5625.238	0	5	3	1	−4.16	6228.598	0	0	0	3	−13.82
7567.112	1	6	6	0	+2.28	8034.720	1	7	1	0	−4.30	7215.971[a]	0	10	8	0	−14.03
6644.127	0	9	9	0	+2.18	4911.832	0	4	2	1	−4.45	7770.008[a]	0	5	5	2	−14.13
7195.678	2	1	1	0	+2.13	9435.375	1	6	0	1	−4.74	6932.932	0	1	1	3	−14.48
7459.459	1	6	4	0	+1.57	7443.402	1	3	1	1	−5.10	7691.774[a]	0	8	4	1	−14.62
2802.959	0	4	0	0	+1.50	4905.650	0	7	3	0	−5.15	5571.734	0	2	0	2	−14.77
3498.086	0	5	1	0	+1.27	6452.263	0	6	6	1	−5.16	6336.631	0	9	5	0	−14.96
4375.376	0	6	6	0	+1.15	6086.264	1	1	1	1	−5.24	9381.428[a]	1	9	3	0	−15.37
7393.467	1	6	2	0	+0.99	2161.615	0	3	3	0	−5.29	6936.836	0	7	1	1	−15.60
8585.581	2	0	0	1	+0.99	8880.764	1	8	6	0	−5.31	7624.871[a]	0	8	2	1	−16.07
3543.625	0	5	3	0	+0.93	6344.487	0	6	4	1	−5.62	7039.129[a]	0	4	4	2	−16.39
2827.134	0	4	2	0	+0.89	1435.440	0	2	2	0	−5.68	9335.679[a]	1	9	1	0	−16.56
5369.820	1	3	1	0	+0.75	6278.422	0	6	2	1	−5.80	7600.536[a]	0	8	0	1	−16.71
8519.393	2	3	1	0	+0.45	4859.669	0	7	1	0	−6.08	5594.851	0	2	2	2	−16.87
7369.444	1	6	0	0	+0.26	7455.423	1	0	0	2	−6.15	6246.878	0	9	3	0	−16.87
7412.993	0	10	10	0	+0.21	6254.406	0	6	0	1	−6.18	6314.119	0	3	3	2	−17.59
4007.098	1	1	1	0	−0.08	4204.148	0	3	1	1	−6.37	7968.884[a]	0	11	9	0	−17.61
6843.879	1	5	5	0	−0.08	8910.898	1	5	5	1	−6.49	6200.333	0	9	1	0	−17.84
4265.998	0	6	4	0	−0.68	8969.988[a]	0	12	12	0	−6.71	7061.078[a]	0	10	6	0	−19.96
5393.698	1	0	0	1	−0.73	5728.750	0	8	6	0	−6.78	8728.056[a]	0	12	10	0	−21.13
2116.414	0	3	1	0	−0.85	5711.723	0	5	5	1	−7.49	6949.074[a]	0	10	4	0	−22.34
3631.473	0	5	5	0	−1.06	6760.705	1	2	0	1	−7.80	6880.434[a]	0	10	2	0	−23.62
4198.983	0	6	2	0	−1.23	8772.080	1	8	4	0	−8.02	6855.443	0	10	0	0	−24.16
8167.247	1	7	5	0	−1.53	7069.720	0	7	5	1	−8.35	7791.506[a]	0	11	7	0	−24.74
4174.609	0	6	0	0	−1.63	2808.518	0	1	1	1	−8.37	7656.971[a]	0	11	5	0	−27.68
8780.819	1	5	1	1	−1.86	4173.071	0	0	0	2	−8.38	7565.908[a]	0	11	3	0	−29.15
4684.310	1	2	0	0	−1.97	7641.128	0	5	1	2	−8.69	8527.968[a]	0	12	8	0	−29.17
8825.250	1	5	3	1	−2.09	6784.172	1	2	2	1	−8.82	7518.738[a]	0	11	1	0	−29.86
7876.854	2	2	2	0	−2.17	8196.387	1	4	4	1	−8.83	8370.673[a]	0	12	6	0	−32.72
8107.969	1	4	0	1	−2.29	3502.121	0	2	0	1	−8.87	9270.461[a]	0	13	9	0	−33.26
7853.511	2	2	0	0	−2.32	6951.683	0	4	0	2	−9.30	8256.910[a]	0	12	4	0	−34.34
6126.351	1	4	4	0	−2.36	7685.158	0	5	3	2	−9.56	8187.207[a]	0	12	2	0	−35.29
8131.572	1	4	2	1	−2.62	6982.219	0	7	3	1	−9.66	8161.892[a]	0	12	0	0	−35.66
7951.843[a]	0	8	8	1	−2.73	8705.445	1	8	2	0	−9.67	9090.108[a]	0	13	7	0	−37.46
8188.274	0	11	11	0	−2.80	4977.196	0	4	4	1	−9.79	8953.319[a]	0	13	5	0	−39.30
4708.059	1	2	2	0	−2.99	5618.181	0	8	4	0	−9.90	8860.739[a]	0	13	3	0	−40.30
8079.988	1	7	3	0	−3.01	7487.510	1	3	3	1	−9.91	8812.732[a]	0	13	1	0	−40.83
7198.969	0	7	7	1	−3.41	6975.047[a]	0	4	2	2	−10.11						

[a]Calculated using predicted spectroscopic constants. The estimated error of the predicted states is less than 1 cm^{-1}.

Table 2. Fitting parameters used to fit the partition functions, see equation (1). Fits are valid for temperatures above 300 K.

	Total	HCN	HNC[a]
a_0	−559.993 791 894	−200.584 273 948	2842.407 266 27
a_1	1208.586 146 39	395.680 813 523	−5546.452 8922
a_2	−1078.942 071 51	−286.330 387 905	4478.672 818 11
a_3	511.994 042 45	71.954 379 5015	−1913.153 845 32
a_4	−136.181 471 79	19.320 519 1562	455.743 140 053
a_5	19.255 610 7068	−17.803 551 7288	−57.362 270 648
a_6	−1.1298 708 2345	4.905 079 546 35	2.978 749 909
a_7	0	−0.624 341 529 866	0
a_8	0	0.030 870 794 9056	0

[a]Partition function given relative to the HNC ground state.

An important parameter in thermal environments, such as the atmospheres of cool stars, is the equilibrium constant, $K(T)$, between HCN and HNC. Barber et al. (2002) estimated this using their partition function. Given the new value of for the energy difference between HCN and HNC used here, one would expect this value to shift. We have therefore re-calculated K as a function of temperature using the HCN and HNC partition functions given in Table 2 and an energy separation of 5705 cm^{-1}. The results are given in Table 3. The increased energy separation results in a reduction in the proportion of HNC by about 25 per cent in the key temperature range of 2000–3000 K compared to the earlier value of Barber et al. (2002).

2.4 Line list calculations

In principle, having substituted the energy levels, the line list is automatically generated using the transitions file. In practice, one more refinement needed to be made. The re-ordering of the energy levels and the shift in the HNC ground state energy led a small minority of transitions whose upper and lower state energies are now inverted giving rise to unphysical transitions with negative frequencies. Since all of these transitions are poorly characterized ones between high-energy states, they were simply removed from the transitions file.

3 RESULTS

Samples of the revised states and transitions files are given in Tables 4 and 5, respectively. Full versions of these files can be downloaded from the Strasbourg data centre, CDS, via ftp://cdsarc.u-strasbg.fr/pub/cats/J/MNRAS/ or from the ExoMol website, www.exomol.com.

Fig. 1 gives an overview of the line list at room temperature, 296 K, in comparison with the, largely experimental, data in HITRAN data base (Rothman et al. 2013). HITRAN only contains HCN, which itself is not an important atmospheric species. It is clear that HITRAN does not give a complete representation of HCN spectral data and, in particular, is missing bands in the region of 4 μm, associated with the $\nu_1 - \nu_2$ difference band, at about 2600 cm^{-1}, and the $\nu_2 + \nu_3$ combination band, near 2800 cm^{-1}.

Fig. 2 gives an expanded view of the regions covering the HCN bending fundamental, ν_2, and overtone, $2\nu_2$. Unsurprisingly, there is excellent agreement between the frequencies in our new line

Table 3. Equilibrium constant K, for HCN ↔ HNC as a function of temperature. The percentage of HNC present in a thermalized sample is also given.

T (K)	$K(T)$	Per cent HNC
800	0.000 05	0.005
850	0.000 10	0.010
900	0.000 18	0.018
950	0.000 29	0.029
1000	0.000 46	0.046
1100	0.000 97	0.097
1200	0.001 88	0.19
1300	0.003 23	0.32
1400	0.005 23	0.52
1500	0.007 89	0.78
1600	0.011 36	1.12
1700	0.015 70	1.55
1800	0.020 89	2.05
1900	0.027 12	2.64
2000	0.034 26	3.31
2100	0.042 37	4.06
2200	0.051 31	4.87
2300	0.061 17	5.75
2400	0.071 75	6.68
2500	0.083 04	7.64
2600	0.094 89	8.63
2700	0.107 32	9.64
2800	0.120 12	10.66
2900	0.133 28	11.67
3000	0.146 67	12.68
3100	0.160 24	13.68
3200	0.173 91	14.65
3300	0.187 59	15.60
3400	0.201 24	16.53
3500	0.214 82	17.43
3600	0.228 25	18.29
3700	0.241 52	19.12
3800	0.254 58	19.93
3900	0.267 40	20.69
4000	0.279 98	21.43

Table 4. Extract from the states file.

I	$\tilde{E}$	g	J	parity	iso	v_1	v_2	l_2	v_3
1	0.000000	6	0	+	0	0	0	0	0
2	1411.413 450	6	0	+	0	0	2	0	0
3	2096.845 540	6	0	+	0	0	0	0	1
4	2802.958 740	6	0	+	0	0	4	0	0
5	3311.477 080	6	0	+	0	0	1	0	0
6	3502.121 100	6	0	+	0	0	2	0	1

I: state counting number; $\tilde{E}$: state energy in cm^{-1}; g: state degeneracy; J: state rotational quantum number; parity: total parity of the state: + or −; iso: isomer label, 0 is HCN, 1 is HNC, 2 is unspecified; v_1: ν_1 state vibrational quantum number; v_2: ν_2 state vibrational quantum number; l_2: vibrational angular momentum associated with ν_2; v_3: ν_3 state vibrational quantum number.

Table 5. Extracts from the transitions file.

I	F	A_{IF}
31 545	29 398	7.7150e−10
139 218	136 884	6.1040e−06
112 117	110 541	1.8330e−04
161 475	160 713	1.1600e−04
76 389	74 341	1.0340e+01
70 455	74 326	6.8550e−04

I: upper state counting number; F: lower state counting number; A_{IF}: Einstein A coefficient in s^{-1}.

list and those in HITRAN as they are based fully on Mellau's data. The agreement between the line intensities is also excellent, proving again our conclusion regarding the accuracy of the ab initio intensities. Our line list indicates the presence of many weak lines, which appear as 'grass' in the expanded scale spectrum in Fig. 2, which are absent from HITRAN. These lines can be associated with hot bands and are significantly more intense at higher temperatures.

While there are many laboratory studies of the spectra of room temperature HCN and HNC, studies of hot spectra are much rarer. Mellau's emission spectra do not contain absolute intensity information and the line frequencies in our line list agree with these experimental measurements by construction, so a comparison is not informative. Maki et al. (2000) recorded an emission spectrum of HCN at about 1370 K. The intensities in this spectrum are subject to self-absorption by cooler HCN but a comparison, as given in Fig. 3 is still useful. Again, although intensities disagree in details for the reasons given above, the overall structure of the two spectra are very similar.

4 CONCLUSIONS

We present a new line list which should produce hot HCN and HNC spectra with significantly improved wavelengths. In particular, the Q-branches, which give sharp spikes in the spectrum, should now be correctly located. As these features are likely to provide the key to any detection of HCN in extrasolar planets, something that is very much expected (Moses 2013), we believe that the improved line list should provide the necessary spectroscopic data. The new line list may be accessed via www.exomol.com or http://cdsarc.u-strasbg.fr/viz-bin/qcat?J/MNRAS/. The states and transitions files may be used to compute temperature-dependent spectra. Alternatively, the ExoMol website provides a facility for generating these data as temperature-dependent cross-sections (Hill, Yurchenko & Tennyson 2013).

Finally, we note that the procedure used here can be employed to improve the wavelengths in any of the line lists generated as part of the ExoMol project. The use of the MARVEL (Measured Active Rotational-Vibrational Energy Levels; Furtenbacher et al. 2007) provides the means of inverting laboratory measurements to give reliable energy levels which can be actively improved as new studies become available. The results of such MARVEL studies can then be used to update the relevant levels file. This procedure was used, at least in part, for water in the latest release of HITEMP (Rothman et al. 2010); and is likely to be used for other line lists in the future.

ACKNOWLEDGEMENTS

This work is supported by ERC Advanced Investigator Project 267219. JKS thanks the Nuffield Foundation for funding under the Nuffield Research Placement Scheme.

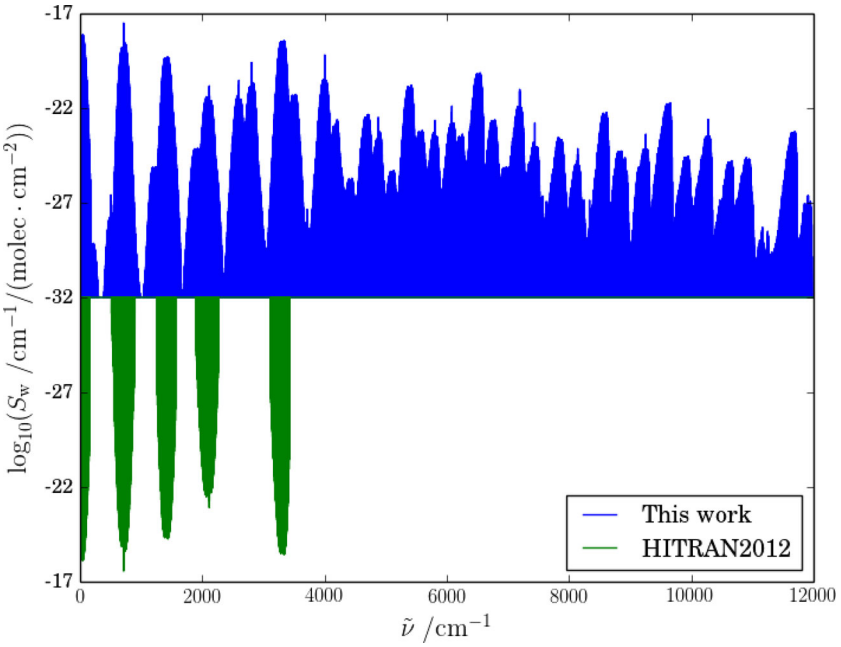

Figure 1. Overview comparison of our line list with the data in HITRAN 2012 (Rothman et al. 2013).

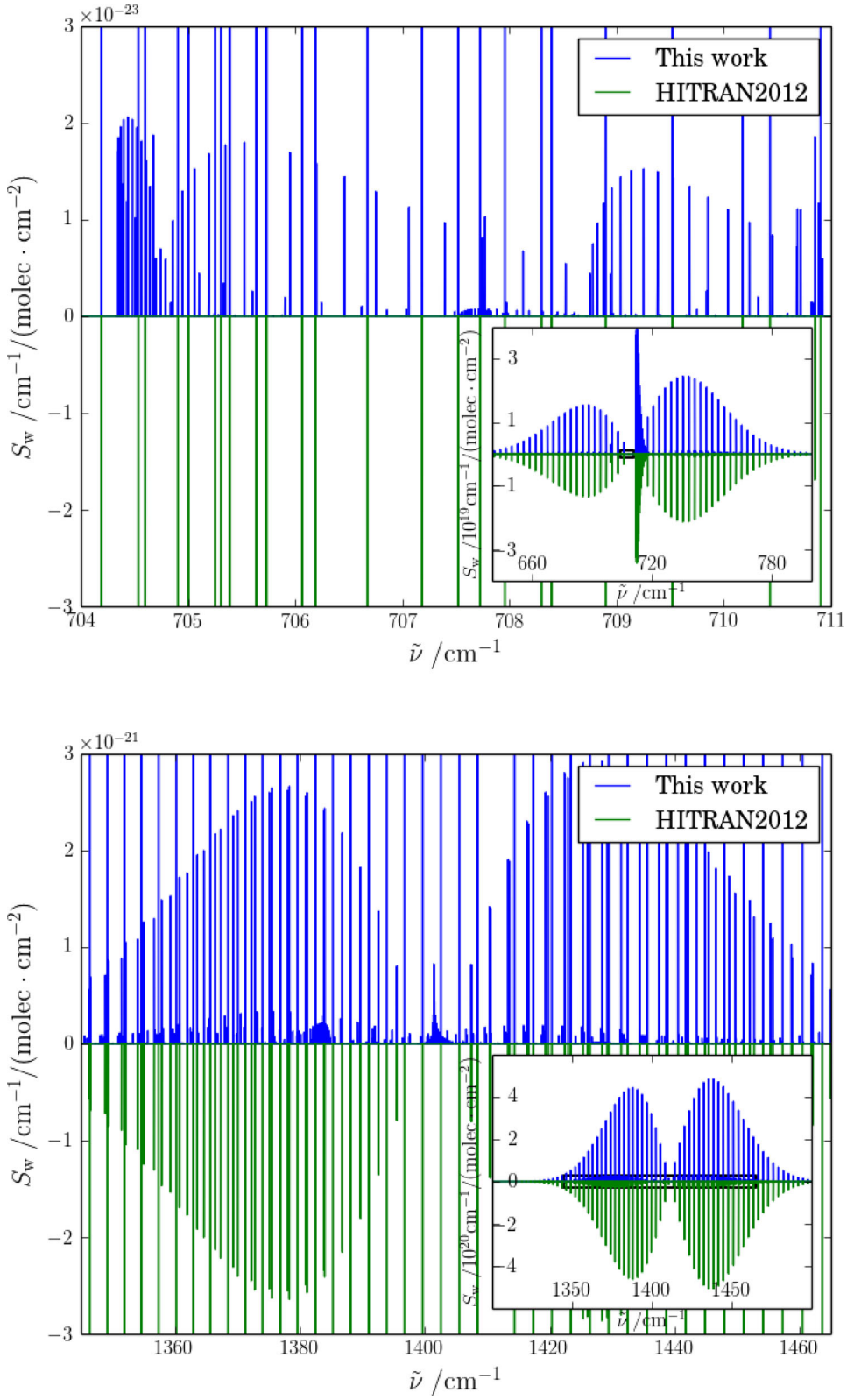

Figure 2. Comparison of our line list with the data in HITRAN 2012 (Rothman et al. 2013) for the region of the ν_2 band (upper) and $2\nu_2$ band (lower).

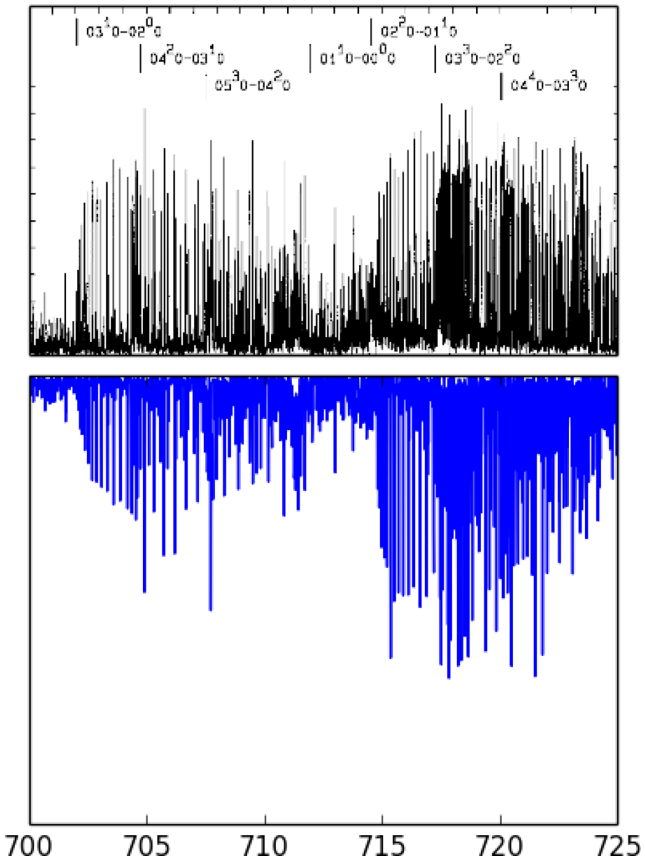

Figure 3. Comparison of our line list with the emission spectra of Maki et al. (2000) assuming a temperature of 1370 K. The first lines of several *Q*-branches are indicated at the top of the figure.

REFERENCES

Barber R. J., Harris G. J., Tennyson J., 2002, J. Chem. Phys., 117, 11239
Barton E. J., Yurchenko S. N., Tennyson J., 2013, MNRAS, 434, 1469
Carr J. S., Najita J. R., 2011, ApJ, 733, 102
Dawes R., Wagner A. F., Thompson D. L., 2009, J. Phys. Chem. A, 113, 4709
Eriksson K., Gustafsson B., Jørgensen U. G., Nordlund A., 1984, A&A, 132, 37
Furtenbacher T., Császár A. G., Tennyson J., 2007, J. Mol. Spectrosc., 245, 115
Harris G. J., Polyansky O. L., Tennyson J., 2002a, Spectrochim. Acta A, 58, 673
Harris G. J., Polyansky O. L., Tennyson J., 2002b, ApJ, 578, 657
Harris G. J., Pavlenko Y. V., Jones H. R. A., Tennyson J., 2003, MNRAS, 344, 1107
Harris G. J., Tennyson J., Kaminsky B. M., Pavlenko Y. V., Jones H. R. A., 2006, MNRAS, 367, 400
Harris G. J., Larner F. C., Tennyson J., Kaminsky B. M., Pavlenko Y. V., Jones H. R. A., 2008, MNRAS, 390, 143
Hill C., Yurchenko S. N., Tennyson J., 2013, Icarus, 226, 1673
Hirota T., Yamamoto S., Mikami H., Ohishi M., 1998, ApJ, 503, 717
Hirota T., Yamamoto S., Kawaguchi K., Sakamoto A., Ukita N., 1999, ApJ, 520, 895
Jørgensen U., Almlöf J., Gustafsson B., Larsson M., Siegbahn P., 1985, J. Chem. Phys., 83, 3034
Lippi M., Villanueva G. L., DiSanti M. A., Boehnhardt H., Mumma M. J., Bonev B. P., Prialnik D., 2013, A&A, 551, A51
Lodi L., Tennyson J., Polyansky O. L., 2011, J. Chem. Phys., 135, 034113
Lynas-Gray A. E., Miller S., Tennyson J., 1995, J. Mol. Spectrosc., 169, 458
Madhusudhan N., 2012, ApJ, 758, 36
Maki A. G., Mellau G. C., Klee S., Winnewisser M., Quapp W., 2000, J. Mol. Spectrosc., 202, 67
Matsuura M. et al., 2005, A&A, 434, 691
Mellau G. C., 2010a, J. Chem. Phys., 133, 164303
Mellau G. C., 2010b, J. Mol. Spectrosc., 264, 2
Mellau G. C., 2011a, J. Chem. Phys., 134, 194302
Mellau G. C., 2011b, J. Chem. Phys., 134, 234303
Mellau G. C., 2011c, J. Mol. Spectrosc., 269, 12
Mellau G. C., 2011d, J. Mol. Spectrosc., 269, 77
Mellau G. C., Winnewisser B. P., Winnewisser M., 2008, J. Mol. Spectrosc., 249, 23
Moses J. I., 2013, Phil. Trans. R. Soc. A, preprint (arXiv:1307.5450)
Moses J. I., Madhusudhan N., Visscher C., Freedman R. S., 2013, ApJ, 763, 25
Oppenheimer B. R. et al., 2013, ApJ, 768, 24
Pau C. F., Hehre W. J., 1982, J. Phys. Chem., 86, 321
Rezac L., Kutepov A. A., Faure A., Hartogh P., Feofilov A. G., 2013, A&A, 555, A122
Rothman L. S. et al., 2010, J. Quant. Spectrosc. Radiat. Transfer, 111, 2139
Rothman L. S. et al., 2013, J. Quant. Spectrosc. Radiat. Transfer, 130, 4
Tennyson J., Yurchenko S. N., 2012, MNRAS, 425, 21
Tinetti G. et al., 2012, Exp. Astron., 34, 311
van Loon J. T., Marshall J. R., Cohen M., Matsuura M., Wood P. R., Yamamura I., Zijlstra A. A., 2006, A&A, 447, 971
van Mourik T., Harris G. J., Polyansky O. L., Tennyson J., Császár A. G., Knowles P. J., 2001, J. Chem. Phys., 115, 3706
Venot O., Hebrard E., Agundez M., Dobrijevic M., Selsis F., Hersant F., Iro N., Bounaceur R., 2012, A&A, 546, A43
Vidler M., Tennyson J., 2000, J. Chem. Phys., 113, 9766
Yadin B., Veness T., Conti P., Hill C., Yurchenko S. N., Tennyson J., 2012, MNRAS, 425, 34

This paper has been typeset from a TEX/LATEX file prepared by the author.